IAEA
International Atomic Energy Agency
Atoms for Peace

24th IAEA Fusion Energy Conference
8-13 October 2012, San Diego, USA

IAEA-CN-197/ TH/8-1

Turbulence spectra, transport, and ExB flows in helical plasmas

T.-H. Watanabe, M. Nunami, H. Sugama, S. Satake, S. Matsuoka,
A. Ishizawa, S. Maeyama and K. Tanaka

NIFS-1038

Nov. 15, 2012

Turbulence spectra, transport, and $\boldsymbol{E} \times \boldsymbol{B}$ flows in helical plasmas

T.-H. Watanabe[1,2], M. Nunami[1,2], H. Sugama[1,2], S. Satake[1,2], S. Matsuoka[1], A. Ishizawa[1,2], S. Maeyama[3] and K. Tanaka[1]

[1]National Institute for Fusion Science, Toki, Gifu 509-5292, Japan
[2]The Graduate University for Advanced Studies, Toki, Gifu 509-5292, Japan
[3]Japan Atomic Energy Agency, Rokkasho, Aomori 039-3212, Japan

Corresponding Author: watanabe.tomohiko@nifs.ac.jp

Abstract:
Gyrokinetic simulation of ion temperature gradient turbulence and zonal flows for helical plasmas has been validated against the Large Helical Device experiments with high ion temperature, where a reduced modeling of ion heat transport is also considered. It is confirmed by the entropy transfer analysis that the turbulence spectrum elongated in the radial wavenumber space is associated with successive interactions with zonal flows. A novel multi-scale simulation for turbulence and zonal flows in poloidally-rotating helical plasmas has demonstrated strong zonal flow generation by turbulence, which implies that turbulent transport processes in non-axisymmetric systems are coupled to neoclassical transport through the macroscopic $\boldsymbol{E} \times \boldsymbol{B}$ flows determined by the ambipolarty condition for neoclassical particle fluxes.

1 Introduction

Inhomogeneity of density and temperature distribution in toroidal plasmas drives turbulent transport of particle, momentum, and heat. Theoretical or numerical evaluation and prediction of the anomalous transport have been a central issue in the magnetic confinement fusion research. Non-axisymmetry in toroidal plasma confinement leads to further complexities in the numerical modeling, and still remains as one of charanges in gyrokinetic simulations of plasma turbulence.

Turbulent transport and zonal flows in helical systems, such as the Large Helical Device [1], have advanced in the last several years. The zonal flow response enhancement by optimization of helical confinement field [2, 3, 4] and the resultant turbulent transport reduction [5, 6] are clarified by the gyrokinetic theory and simulation. The long-time response function of zonal flows is also amplified by the equilibrium scale radial electric field [7, 8, 9] which is spontaneously generated by the ambipolar particle diffusion of the neoclassical transport and drives a poloidal $\boldsymbol{E} \times \boldsymbol{B}$ rotation. The zonal flow enhancement is associated with improvement of collisionless orbits of helical ripple trapped particles, and couples the anomalous and neoclassical transport processes.

In this paper, we report recent progresses in the gyrokinetic simulation study of the LHD plasma. The flux tube gyrokinetic code, GKV-X [10, 11], which incorporates the equilibrium field reconstructed from the LHD experimental data, is applied to simulation of the ion temperature gradient (ITG) turbulence [12]. The simulation results show a reasonable agreement in the anomalous transport flux with the experimental ones, which is the first validation of the gyrokinetic simulation against the helical plasma experiments. We have recently performed a series of simulation runs for LHD equilibria of the high ion temperature (T_i) discharge or the inward-shifted magnetic axis configuration. The obtained result manifests a simple relation among the transport coefficient, the turbulence intensity, and the zonal flow amplitude.

It is widely accepted that zonal flows play a crucial role in reduction of the heat transport in the ITG turbulence. The turbulence regulation by zonal flows is quantitatively analyzed by means of the nonlinear entropy transfer function [13]. We apply the entropy transfer analysis to the ITG turbulence simulation for the LHD experimental configuration.

The zonal flow response enhancement by the radial electric field has been simulated with a (poloidally) global model [9, 14, 15, 16] including a field line label dependence of the confinement field strength. Application of the poloidally global model to the ITG turbulence, however, causes a difficulty, that is, mixture of different scale lengths for equilibrium and turbulence. To overcome this issue, we have devised a multi-scale simulation model for turbulence and zonal flows in helical plasmas with the poloidal $\boldsymbol{E} \times \boldsymbol{B}$ rotation.

The present paper is organized as follows. In section 2, results of the GKV-X simulation for the high-T_i LHD plasmas are presented in comparison with LHD experiments, and a scaling model of the transport coefficient is considered. Fluctuation spectra obtained by the ITG turbulence simulations for the LHD high-T_i discharge are also discussed by means of the entropy transfer function. A multi-scale simulation result of the ITG turbulence and zonal flows is shown in section 3, where one finds strong zonal flow generation by the ITG turbulence in case with the equilibrium-scale poloidal rotation. A summary is given in the last section.

2 Gyrokinetic simulations for LHD plasmas with high T_i

2.1 Turbulent transport and zonal flows

The gyrokinetic simulation using GKV-X code enables us quantitative evaluation of the ITG turbulent transport in the LHD plasma with high ion temperature. The electrostatic turbulence simulations with the gyrokinetic ions and adiabatic electron response are carried out for different flux surfaces of which equilibrium configuration is reconstructed by the VMEC code [17] for the LHD experiment. In the high-T_i experiments, the phase contrast imaging (PCI) measurement [18] has detected density fluctuations with a dispersion relation relevant to the ITG mode [19]. The radial location where large density fluctuations were observed is also consistent with the ITG unstable region predicted by the gyrokinetic simulations. Comparison of the ion heat fluxes P_{i} obtained from the simulations and the LHD experiment (#88343) is plotted in FIG.1 (left), where the simulation results obtained for five different minor radii (ρ) show reasonable agreement with the anomalous ion heat flux (solid line) obtained by subtracting the numerically-evaluated neoclassical part from the experimental values (dotted line).

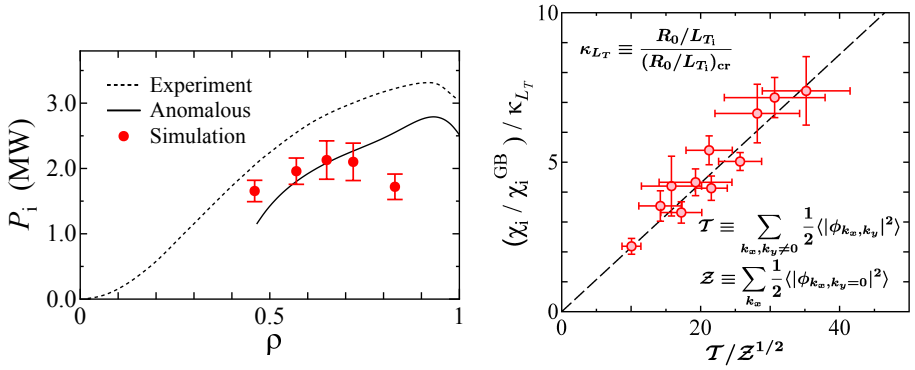

Figure 1: (Left) Ion heat transport flux P_i obtained by the GKV-X simulation (solid circles) compared with the high-T_i LHD experiments, where the anomalous part is shown by solid line. (Right) A summary of χ_i obtained by simulations for the high-T_i and the inward-shifted magnetic axis cases.

The ion heat transport coefficient resulting from the GKV-X simulations for the high-T_i discharge and the inward-shifted magnetic axis configurations are summarized in FIG. 1 (right), where the vertical axis is normalized by the gyro-Bohm diffusion coefficient, $\chi_i^{GB} = \rho_{ti}^2 v_{ti}/R_0$, and a ratio of the ion temperature gradient to the critical value, $\kappa_{L_T} = (R_0/L_T)/(R_0/L_T)_{cr}$. Each mark represents the time-averaged value, where the error bars mean their root-mean-square of the time variations. The horizontal axis of FIG. 1 (right) is defined by the ratio of turbulence energy and the mean zonal flow amplitude, that is, $\mathscr{T}/\mathscr{Z}^{1/2}$, where $\mathscr{T} \equiv (1/2)\sum_{k_x,k_y\neq 0}\langle|e\phi_{k_x,k_y}R_0/T_i\rho_{ti}|^2\rangle$ and $\mathscr{Z} \equiv (1/2)\sum_{k_x}\langle|e\phi_{k_x,0}R_0/T_i\rho_{ti}|^2\rangle$. Average along the field line is denoted by $\langle\cdots\rangle$. One clearly finds a linear relationship between the horizontal and vertical quantities, even for the different radial positions and the helical components of confinement field. We have also found that $\mathscr{T}$ and $\mathscr{Z}$ can be related to the linear ITG growth rates and the zonal flow response function, respectively. The obtained result is expected to contribute to a reduced transport modeling which enables us to estimate a turbulent ion heat diffusivity for high-T_i LHD plasma from linear calculations of the ITG mode and the zonal flow response.

2.2 Fluctuation spectra and entropy transfer

The self-generated zonal flows causing turbulence regulation spread the fluctuation spectrum into the higher radial wavenumber space [12]. Power spectra of the electrostatic potential at $\theta = 0$ (θ : $poloidalangle)forthehigh-T_i$ LHD discharge are plotted in the two-dimensional wavenumber space in FIG. 2, where $\rho = 0.46$ (left) and 0.83 (right). The fluctuation spectrum for $\rho = 0.83$ is elongated in the higher radial wavenumber (k_x) region where the ITG mode is linearly stable. In contrast, the spectrum for $\rho = 0.46$ shows a more isotropic profile in the k_x-k_y space. The difference is attributed to the zonal flow generation, where the zonal flow potential energy $\mathscr{Z}$ at $\rho = 0.83$ is about ten times larger than that for $\rho = 0.46$, while χ_i/χ_i^{GB} is comparable for the two cases even with one order higher level of turbulent fluctuation energy $\mathscr{T}$ at $\rho = 0.83$ [12].

The spreading of turbulent fluctuation spectrum into the high-k_x components with less trans-

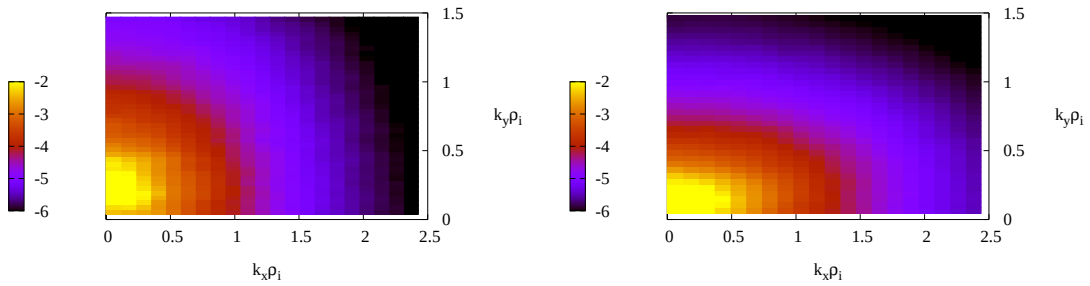

Figure 2: Power spectrum of electrostatic potential fluctuations at $\theta = 0$ *obtained from the GKV-X simulations for* $\rho = 0.46$ *(left) and* 0.83 *(right), respectively, where the time average is taken for* $60R_0/v_{ti} < t < 100R_0/v_{ti}$ *(left) and* $40R_0/v_{ti} < t < 90R_0/v_{ti}$ *(right).*

port efficiency is explained by the successive entropy transfer process through triad interactions of zonal flows and turbulence [13]. The previous entropy transfer analysis applied to the model LHD configurations for the standard and the inward-shifted cases demonstrates that larger transfer of the entropy variable occurs in the later case with stronger zonal flows [20]. The entropy transfer function is defined by a quadratic integral of the perturbed ion gyrocenter distribution function, such that,

$$\mathscr{J}\left[\boldsymbol{p}_\perp \,|\, \boldsymbol{q}_\perp, \boldsymbol{k}_\perp\right] = \left\langle \boldsymbol{b}\cdot(\boldsymbol{q}_\perp \times \boldsymbol{k}_\perp) \int d^3v \frac{1}{2F_M} \mathrm{Re}\left[\Phi_{\boldsymbol{q}_\perp} h_{\boldsymbol{k}_\perp} h_{\boldsymbol{p}_\perp} - \Phi_{\boldsymbol{k}_\perp} h_{\boldsymbol{q}_\perp} h_{\boldsymbol{p}_\perp}\right] \right\rangle . \qquad (1)$$

The entropy transfer function with the triad interaction condition, $\delta_{\boldsymbol{k}_\perp+\boldsymbol{p}_\perp+\boldsymbol{q}_\perp,0}\overline{\mathscr{J}}\left[\boldsymbol{p}_\perp \,|\, \boldsymbol{q}_\perp, \boldsymbol{k}_\perp\right]$, is plotted in FIG. 3 for the cases with $\rho = 0.46$ and 0.83, where $\overline{\cdots}$ means a time average. The mode with the wavenumber $\boldsymbol{p}_\perp$ is chosen to be one of the dominant turbulent components, that is, $\boldsymbol{p}_\perp \rho_i = (0.231, 0.210)$ and $(0.244, 0.127)$ for $\rho = 0.46$ and 0.83, respectively. The entropy transfer to the mode with $\boldsymbol{p}_\perp$ is represented by the red color, and is typically found at $\boldsymbol{q}_\perp \rho_i = (0, -0.127)$ and $(-0.244, 0)$ for $\rho = 0.83$ in the right panel, while it is randomly distributed for $\rho = 0.46$ shown in the left. The decrease in the entropy of the mode $\boldsymbol{p}_\perp$ is shown by blue, which is found in the higher radial wavenumber region, such as $\boldsymbol{q}_\perp \rho_i = (-0.610, -0.127)$ or higher $|q_x|$ for $\rho = 0.83$. The horizontal striation patten found in the transfer function for $\rho = 0.83$ means the successive entropy transfer process, and is consistent with those found in the ITG turbulence in tokamaks [13] and in the inward-shifted LHD configurations [20]. Therefore, it is concluded that the elongated fluctuation spectrum found in FIG. 2 (right) is caused by the nonlinear interaction among turbulence and strong zonal flows.

3 Multi-scale simulation for helical plasmas with E_r

The neoclassical and turbulent transport simulations provide us a basis for quantitative analysis the transport processes in LHD plasmas. The ambipolar radial electric field with an equilibrium scale-length, $\overline{E}_r$, is estimated by the neoclassical transport analysis code, FORTEC-3D, with the finite orbit width effect [21, 22]. However, effects of the macroscopic poloidal $\boldsymbol{E}\times\boldsymbol{B}$ rotation on zonal flows are not introduced in the conventional flux-tube simulations. While a (poloidally)

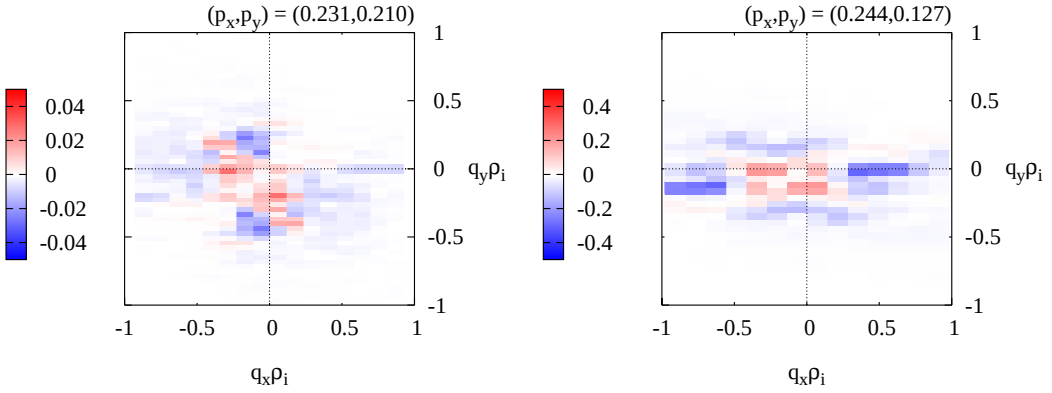

Figure 3: Entropy transfer function $\delta_{\boldsymbol{k}_\perp+\boldsymbol{p}_\perp+\boldsymbol{q}_\perp,0}\overline{\mathscr{J}}\,[\boldsymbol{p}_\perp\,|\,\boldsymbol{q}_\perp,\boldsymbol{k}_\perp]$ *for* $\rho = 0.46$ *(left) and* 0.83 *(right), where wavenumbers of the mode* $\boldsymbol{p}_\perp$ *are* $\boldsymbol{p}_\perp\rho_i = (0.231, 0.210)$ *and* $(0.244, 0.127)$*, respectively. The time-average is the same as those used for FIG.1.*

global model has been applied to the zonal flow response analysis in case with $\overline{E}_r$ [15], a more elaborate model is preferable to treat interactions of disparate scales.

To investigate the coupling of the neoclassical and turbulent transport processes through $\overline{E}_r$ and zonal flows, we have developed a new multi-scale computational model, *flux-tube bundle* model. The multi-scale model consists of several flux tubes for turbulence components and a global zonal-flow mode solver. In each flux tube located at different field line label, the conventional δf gyrokinetic equation is solved where the poloidal rotation term causes the Doppler shift of the mode frequency. The zonal component (shown by $\widehat{\cdots}$) is obtained by solving the gyrokinetic equation derived from retaining the interaction with macroscopic scales through the $\boldsymbol{E}\times\boldsymbol{B}$ rotation,

$$\left[\frac{\partial}{\partial t} + v_\parallel \boldsymbol{b}\cdot\nabla + v_{dx}\frac{\partial}{\partial x} - \frac{\mu}{m}(\boldsymbol{b}\cdot\nabla B)\frac{\partial}{\partial v_\parallel} + \omega_\theta q_0 \frac{\partial}{\partial \alpha}\right]\widehat{f} = \left(-v_{dx}\frac{\partial \widehat{\Phi}}{\partial x} - v_\parallel \boldsymbol{b}\cdot\nabla\widehat{\Phi}\right)\frac{e}{T_i}F_M + C(\widehat{f}) + S^{ZF} \tag{2}$$

where S^{ZF} represents the source term driven by the turbulence, $S^{ZF} = -(c/B_0)\langle\langle\{\Phi,\delta f\}\rangle\rangle_\alpha$. The average over the turbulence scale in the y coordinate is denoted by $\langle\langle\cdots\rangle\rangle_\alpha$.

The zonal flow response to a given source term is calculated by means of the linear gyrokinetic simulation using the flux-tube bundle model. Time-history of the zonal flow potential is plotted in FIG. 4, where M_p means the poloidal Mach number, $M_p = |\omega_\theta|R_0q_0/v_{ti} = (R_0q_0/r_0)|c\overline{E}_r/B_0v_{ti}|$. Eight flux tubes are set in the flux-tube bundle model for a range of $-\pi/M \le \alpha \le +\pi/M$ with $M = 10$ for the LHD configuration, where α means the field line label $\alpha = \zeta - q\theta$ and q is the safety factor. We have employed the same physical parameters as those for the inward-shifted case in Ref. [6]. The residual zonal flow level after the initial damping of the geodesic acoustic mode (GAM) is enhanced by $\overline{E}_r$, which is consistent with the previous simulaitons [15]. As the finite collision term is introduced, the residual zonal flow level decays in a longer time. The macroscopic $\overline{E}_r$ determined by the ambipolar condition of neoclassical particle transport fluxes enhances the zonal flow generation, because the radial

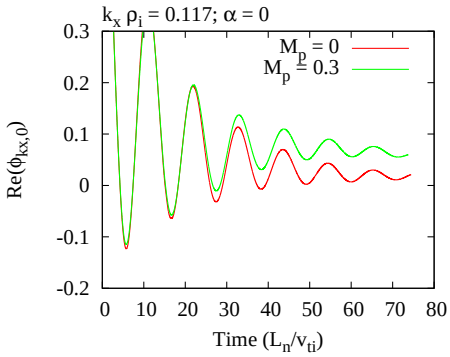

Figure 4: Time history of the zonal flow response calculated by means of the flux-tube bundle model for cases with (red) and without (green) poloidal rotation, where M_p denotes the poloidal Mach number.

drift motion of ripple-trapped particles can be weakened by the $\boldsymbol{E} \times \boldsymbol{B}$ rotation as well as by the neoclassical optimization of the magnetic configuration. The M_p dependence of the zonal flow response suggests an unique property of the helical plasma transport, where the uniform $\overline{E}_r$ without flow shear can induce an isotope effect on the turbulent transport and coupling of the neoclassical and turbulent transport processes.

Nonlinear simulations of the ITG turbulence using the flux-tube bundle model have also been carried out where the eight flux tubes are employed. The physical and numerical parameters are the same as those given above. In case without the poloidal rotation ($M_p = 0$), turbulence and zonal flows in each flux tube develop independently. The total average of the heat flux agrees with that of the single flux tube case, because the ITG mode in LHD plasma has little dependence on the field line label α [23]. In case with the poloidal rotation, a collective phenomenon among different flux tube arises when zonal flows developed in the ITG turbulence. Because of the zonal flow response enhancement by $\overline{E}_r$, the zonal flow amplitudes in the flux tubes continue to grow after the initial saturation of the instability growth as seen in FIG. 5 (left). For $M_p = 0.3$, the zonal flow energy averaged over flux tubes is about two times higher than that for $M_p = 0$. In the collective growth phase of zonal flows, the radial phase angles synchronize with each other, while they were random in the linear stage of the ITG instability. The initial peak value of ion heat transport for $M_p = 0.3$ is about 70% higher than that for $M_p = 0$ [see FIG. 5 (right)], because of less effective regulation of turbulence by zonal flows in the synchronization process. However, the turbulent transport level gradually decreases as the collective growth of zonal flows, and becomes comparable to the case of $M_p = 0$. As further reduction of the turbulent transport is expected in a longer time limit, we would further continue the multi-scale simulation of ITG turbulence and zonal flows in helical systems with $\overline{E}_r$.

4 Summary

Turbulence spectra and transport in helical plasmas are investigated by the gyrokinetic simulations of ion temperature gradient (ITG) turbulence interacting with microscopic $\boldsymbol{E} \times \boldsymbol{B}$ zonal flows. The first validation of the GKV-X code against the high ion temperature discharge of

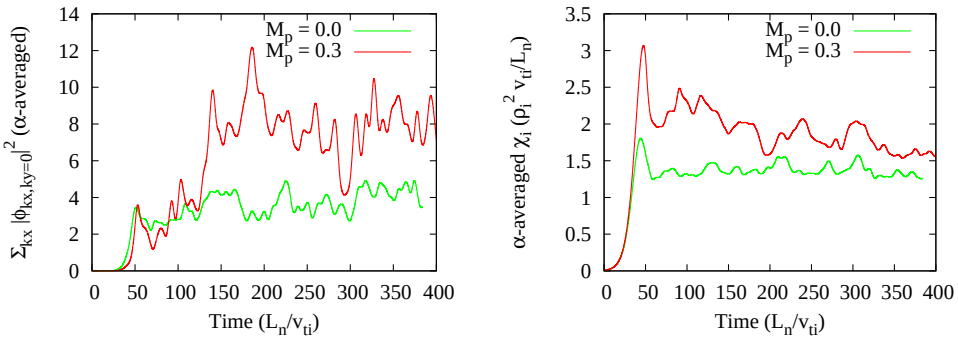

Figure 5: Time history of the zonal flow potential energy (left) and the ion heat transport coefficient averaged over flux tubes in cases with (red) and without (green) poloidal rotation, where M_p denotes the poloidal Mach number.

Large Helical Device (LHD) experiments shows a fair agreement on the turbulent ion heat transport. Results from the gyrokinetic simulations of the ITG turbulence demonstrate a simple relationship among the turbulent transport, the turbulence intensity, and the zonal flow amplitude, and suggest a possible transport modeling for helical systems based on the first principle simulations. The gyrokinetic simulations for the LHD configurations clarify the spectral transfer of potential fluctuations toward stable modes with higher radial wavenumbers through zonal flow-turbulence interactions, which is confirmed by the entropy transfer function.

The macroscopic ambipolar radial electric field $\overline{E}_r$, which is evaluated by the neoclassical transport code, FORTEC-3D, including the finite-orbit-width effects, leads to further enhancement of the zonal flow response. The "flux-tube bundle" model is constructed for the multi-scale simulation of turbulence and zonal flows in case with $\overline{E}_r$ in helical plasmas. The zonal flow response enhancement is reconfirmed by the novel simulation model. The multi-scale simulation of the ITG turbulent transport in helical systems with $\overline{E}_r$ has also been initiated, showing stronger zonal flow generation by turbulence. More detailed investigations on the multi-scale turbulent transport by means of the flux-tube bundle model are currently in progress, and the results will be reported elsewhere.

Acknowledgments

This work is supported in part by grants-in-aid of the Ministry of Education, Culture, Sports, Science and Technology (No. 21560861, 22760660, and 24561030), and in part by the National Institute for Fusion Science (NIFS) Collaborative Research Program (KNTT006, KNST006, and UNTT002). Numerical simulations are carried out by use of the Plasma Simulator system at National Institute for Fusion Science, and by use of Helios system at International Fusion Energy Research Center (Project code: VLDGK and GTNAXIS). A part of this work is carried out during one of the authros (T.-H. W.) stays at the gyrokinetic theory working group meeting held at EURATOM-CIEMAT.

References

[1] Yamada H et al. 2011 *Nucl. Fusion* **51** 094021

[2] Sugama H and Watanabe T H 2005 *Phys. Rev. Lett.* **94** 115001

[3] Sugama H and Watanabe T H 2006 *Phys. Plasmas* **13** 012501

[4] Ferrando-Margalet S, Sugama H and Watanabe T H 2007 *Phys. Plasmas* **14** 122505

[5] Watanabe T H, Sugama H. and Ferrando-Margalet S. 2007 *Nucl. Fusion* **47** 1383

[6] Watanabe T H, Sugama H and Ferrando-Margalet S 2008 *Phys. Rev. Lett.* **100** 195002

[7] Sugama H, Watanabe T H and Ferrando-Margalet S 2008 Plasma Fus. Res. **3** 041

[8] Sugama H and Watanabe T H 2009 *Phys. Plasmas* **16** 056101

[9] Sugama H, Watanabe T H and Nunami M 2010 *Contrib. Plasma Phys.* **50**, 571-575

[10] Nunami M, Watanabe T H, and Sugama H 2010 *Plasma Fusion Res.* **5** 016

[11] Nunami M, Watanabe T H, Sugama H, and Tanaka K 2011 *Plasma Fusion Res.* **6** 1403001

[12] Nunami M, Watanabe T H, Sugama H and Tanaka K 2012 *Phys. Plasmas* **19** 042504.

[13] Nakata M, Watanabe T H and Sugama H 2012 *Phys. Plasmas* **19** 022303

[14] Kleiber R, Hatzky R and Mishchenko A 2010 *Contrib. Plasma Phys.* **50**, 766-769

[15] Watanabe T H, Sugama H and Nunami M. 2011 *Nucl. Fusion* **51** 123003

[16] Sánchez E et al. in *The Joint 18th International Stellarator/Heliotron Workshop and 10th Asia Pacific Plasma Theory Conference* (Sydney, Australia, 2012) S2.3Tu

[17] Hirshman S P, Betancourt O 1991 *J Comput Phys* **96** 99

[18] Tanaka K et al 2008 *Rev. Sci. Instrum.* **79** 10E702

[19] Tanaka K et al 2010 *Plasma Fusion Res.* **5** S2053

[20] Watanabe T H, Sugama H, Nunami M, Tanaka K and Nakata M 2012 *Plasma Phys. Control. Fusion* (in press)

[21] Satake S, Sugama H, and Watanabe T H 2007 *Nucl. Fusion* **47** 1258

[22] Matsuoka S, et al 2011 *Plasma Fusion Res.* **6** 1203016

[23] Kuroda T, Sugama H 1998 *J Phys Soc Jpn* **67** 3787